

Thermodynamic Studies on Non Centrosymmetric Superconductors by AC Calorimetry under High Pressures^{*†}

Naoyuki TATEIWA^{1‡}, Yoshinori HAGA¹, Tatsuma D. MATSUDA¹, Etsuji YAMAMOTO¹, Shugo IKEDA¹,
Tetsuya TAKEUCHI², Rikio SETTAI², and Yoshichika ÔNUKI^{1,2}

¹*Advanced Science Research Center, Japan Atomic Energy Agency, Tokai, Ibaraki 319-1195, Japan*

²*Department of Physics, Faculty of Science, Osaka University, Toyonaka 560-0043, Japan*

(Received July 21, 2006)

We investigated the non centrosymmetric superconductors CePt₃Si and UIr by the ac heat capacity measurement under pressures. We determined the pressure phase diagrams of these compounds. In CePt₃Si, the Néel temperature $T_N = 2.2$ K decreases with increasing pressure and becomes zero at the critical pressure $P_{AF} \simeq 0.6$ GPa. On the other hand, the superconducting phase exists in a wider pressure region from ambient pressure to $P_{AF} \simeq 1.5$ GPa. The phase diagram of CePt₃Si is very unique and has never been reported before for other heavy fermion superconductors. In UIr, the heat capacity shows an anomaly at the Curie temperature $T_{C1} = 46$ K at ambient pressure, and the heat capacity anomaly shifts to lower temperatures with increasing pressure. The present pressure dependence of T_{C1} was consistent with the previous studies by the resistivity and magnetization measurements. Previous ac magnetic susceptibility and resistivity measurements suggested the existence of three ferromagnetic phases, FM1-3. C_{ac} shows a bending structure at 1.98, 2.21, and 2.40 GPa. The temperatures where these anomalies are observed are close to the phase boundary of the FM3 phase.

KEYWORDS: CePt₃Si, UIr, superconductivity, ac calorimetry

1. Introduction

Recently, the discovery of non centrosymmetric superconductors such as CePt₃Si, UIr, CeRhSi₃, CeIrSi₃, and CeCoGe₃ has attracted considerable attention from both theoretical and experimental view points.¹⁻⁵ In these compounds, two spin degenerate bands are split due to the Rashba-type spin-orbit interaction, which strongly influences the superconducting properties, particularly the pairing symmetry of the Cooper pairs. Theoretical studies suggest a mixed-type pair function with spin triplet and singlet components.⁶ Many theoretical and experimental studies have been extensively conducted in order to clarify this novel type of unconventional superconductivity. In this paper, we describe our thermodynamic studies on CePt₃Si and UIr under high pressure.

CePt₃Si crystallizes in the tetragonal structure (space group $P4mm$) in which inversion center is absent. Superconductivity is observed at the transition temperature $T_{sc} = 0.75$ K below the Néel temperature $T_N = 2.2$ K at which antiferromagnetism is observed in CePt₃Si.¹ Further, a microscopic coexistence between magnetism and superconductivity was suggested based on the neutron scattering, μ SR and NMR experiments.⁷⁻¹⁰ The finding of the superconductivity led to many theoretical and experimental studies for understanding the novel superconductivity in systems without inversion centers. In the NMR experiment, two superconducting order parameters comprising the spin singlet- and triplet-pairing components have been suggested.¹¹ The previous high-pressure

study by the resistivity measurement showed that the superconducting transition temperature T_{sc} decreases with an increase in the pressure and becomes 0 K at around 1.5 GPa.¹² On the other hand, the pressure dependence of the antiferromagnetic transition temperature T_N is not clear because the anomaly in the resistivity at T_N is too weak to be detected.

UIr is a ferromagnetic compound with the Curie temperature $T_{C1} = 46$ K.^{13,14} UIr crystallizes in the monoclinic PbBi-type structure (space group $P2_1$). There is no inversion center in the crystal structure. The magnetic susceptibility obeys the Curie-Weiss law at temperatures above 500 K, with an effective magnetic moment $\mu_{eff} = 3.6 \mu_B/U$; this value corresponds to the free-ion value of the localized $5f^2$ and/or $5f^3$ configurations. In the ferromagnetic state, the magnetization is highly anisotropic and the magnetic property is of the Ising type. The size of the spontaneous magnetic moment oriented along the $[10\bar{1}]$ direction is $0.5 \mu_B/U$. The cyclotron effective mass in the range of 10 - $30m_0$ was observed in the de Haas van Alphen experiment. The electronic specific heat coefficient was determined to be $\gamma = 49$ mJ/K²·mol.^{15,16} The itinerant character of the $5f$ electrons at low temperatures was suggested. Previous high-pressure studies showed that the Curie temperature T_{C1} decreases with increasing pressure and that superconductivity is observed in a narrow pressure region from 2.6 to 2.7 GPa.^{2,17,18} A recent study revealed the existence of three ferromagnetic phases FM1-3 and that the superconducting phase exists at a pressure just below the critical pressure of the FM3 phase.¹⁹

In order to establish the pressure phase diagram of both the compounds, the thermodynamic measurements are necessary. We carried out the ac heat capacity mea-

^{*}This paper was presented at the international workshop "Novel Pressure-induced Phenomena in Condensed Matter Systems(NP2CMS)" August 26-29 2006, Fukuoka Japan.

[†]J. Phys. Soc. Jpn. **76** (2007) Suppl. A, pp. 140-143

[‡]E-mail: tateiwa.naoyuki@jaea.go.jp

surement on CePt₃Si and UIr under high pressures. We present the experimental results in this paper.

2. Experimental

A single crystal of CePt₃Si was grown by the Bridgman method and that of UIr was grown by the Czochralski method in a tetra-arc furnace. The details of the sample preparation are given in our previous papers.^{12,15} These values of the residual resistivity ratio RRR ($=\rho_{RT}/\rho_0$) are 100 and 200 for CePt₃Si and UIr, respectively. Those values indicate the high quality of the single crystal samples. The ac heat capacity measurement under pressure was measured using a AuFe-Au thermocouple in a hybrid piston cylinder-type cell. The details of experimental techniques for the ac calorimetry are given in ref. [20].

3. Results and discussions

3.1 CePt₃Si

The pressure-temperature phase diagram of CePt₃Si obtained by the heat capacity measurement is shown in Figure 1. The superconducting transition temperatures T_{sc} previously determined by both resistivity ρ and ac susceptibility χ_{ac} measurements are also plotted in the figure.¹² The Néel temperature determined by the resistivity measurement was not plotted because there was ambiguity in the determination of T_N due to the weak resistivity anomaly at the transition temperature. With increasing pressure, T_N decreases faster than T_{sc} and becomes 0 K at around $P_{AF} \simeq 0.6$ GPa. T_{sc} decreases with increasing pressure and becomes approximately constant from 0.6 GPa to 0.8 GPa. It decreases furthermore with increasing pressure and becomes zero at $P_{sc} \simeq 1.5$ GPa. Thus, the pressure dependence of T_{sc} shows a characteristic feature. The present pressure of 0.6 GPa corresponds to the antiferromagnetic critical pressure P_{AF} . CePt₃Si is in the paramagnetic state from $P_{AF} \simeq 0.6$ GPa to 1.5 GPa and it shows only superconducting transitions.

Pressure-induced superconductivity was observed in several cerium compounds such as CeIn₃, CeRh₂Si₂ and

CePd₂Si₂.²¹ These compounds show the antiferromagnetic ordering at ambient pressure. The T_N value decreases with increasing pressure. Superconductivity is observed around the magnetic critical point P_{AF} , where T_N becomes zero. The superconducting phase exists in a narrow pressure region around the antiferromagnetic critical pressure P_{AF} . The T_{sc} value becomes maximum around the critical pressure. Superconductivity is considered to be mediated by the low-energy magnetic excitations around the magnetic quantum critical point P_{AF} . On the other hand, in the case of CePt₃Si, the bulk superconducting phase exists in a wide pressure region above and below P_{AF} , and T_{sc} does not show a maximum at P_{AF} . The maximum T_{sc} value is realized at ambient pressure. From the pressure dependence of the linear heat capacity coefficient γ , it was suggested that the critical pressure P_{AF} is not of the second-order quantum critical point but that of the first-order.²⁰ Therefore, the superconductivity in CePt₃Si may be different from that around the magnetic quantum critical point.

3.2 UIr

Figure 2 shows the temperature dependence of C_{ac} (right side) at ambient pressure. The experimental data obtained by the relaxation method is also plotted (left side). Both the data are scaled around 50 K by experimental data. The temperature dependence of C_{ac} is qualitatively consistent with that obtained by the relaxation method. At ambient pressure, the heat capacity shows an anomaly at around the ferromagnetic transition temperature $T_{C1} = 46$ K.

Figure 3 shows the heat capacity C_{ac} under pressures up to 1.58 GPa. The experimental data under pressures are simply shifted upwards. With increasing pressure, the anomaly at T_{C1} shifts to the lower temperature side and the strength of the anomaly becomes weaker. At 1.58

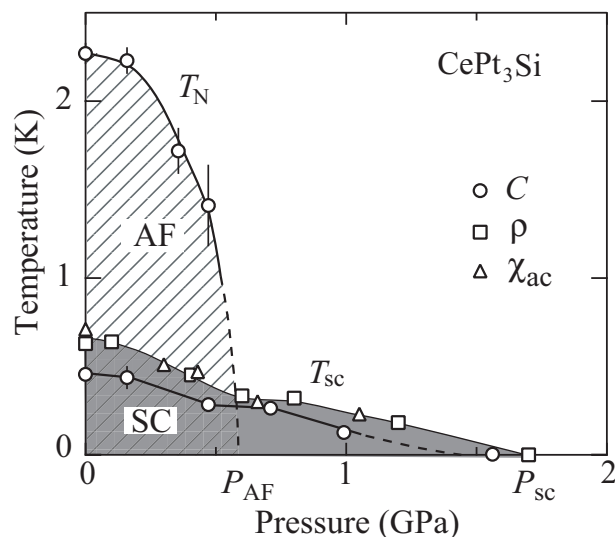


Fig. 1. Pressure phase diagram of CePt₃Si.

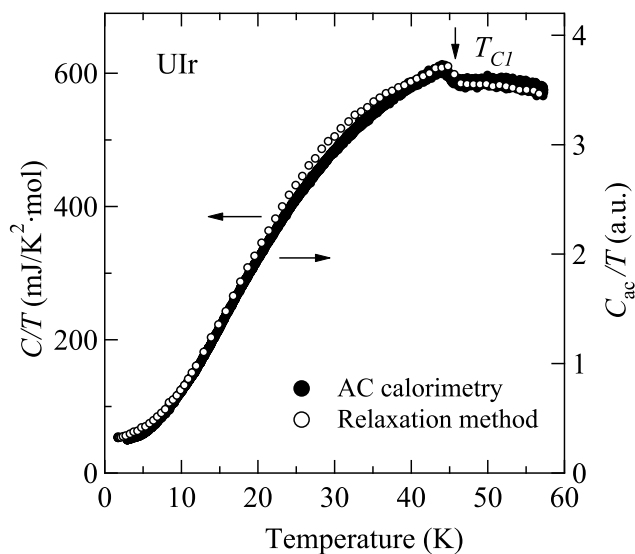


Fig. 2. Temperature dependence of C_{ac} by the present measurement (right side) and the data obtained by the relaxation method (left side).

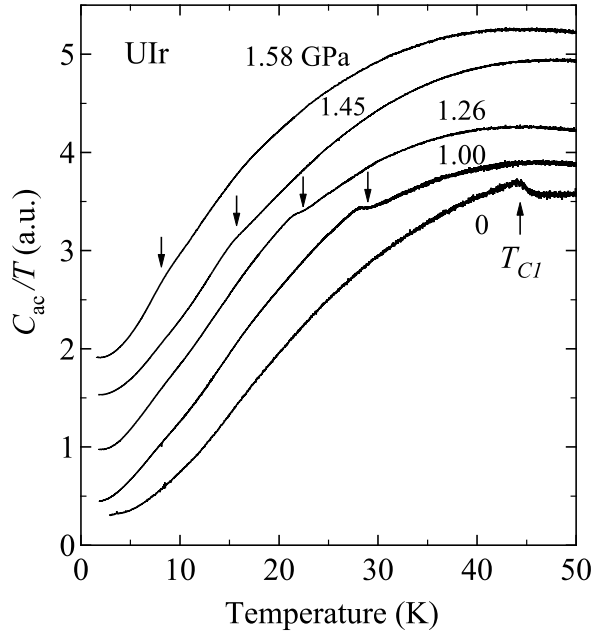


Fig. 3. Temperature dependence of the heat capacity of UIr under high pressures.

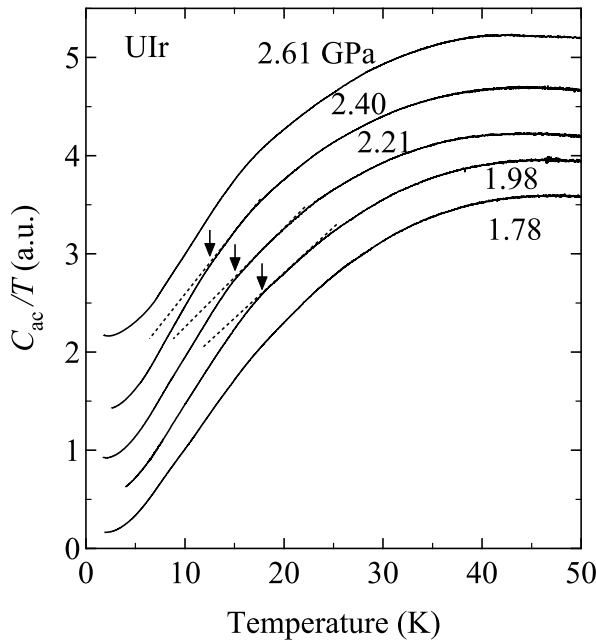


Fig. 4. Temperature dependence of the heat capacity of UIr under high pressures.

GPa, a weak anomaly is observed at around 10 K.

Figure 4 shows the heat capacity C_{ac} in the pressure region from 1.58 GPa to 2.61 GPa. The experimental data under pressures are simply shifted upwards. In this region, there is no distinct heat capacity anomaly. However the curve of C_{ac} at 1.98, 2.21 and 2.40 GPa shows a bending structure as shown in Figure. 4. In the Fig.4, arrows are used to indicate the temperature at which

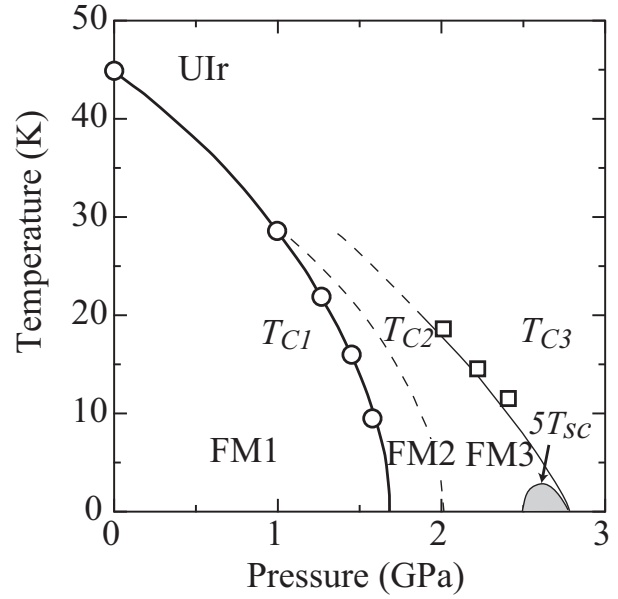


Fig. 5. Pressure phase diagram of UIr

C_{ac} shows bending. As discussed later, the temperatures are close to the phase boundary of the FM3 phase. No anomaly is observed in C_{ac} around the phase boundary of the FM2.

The pressure phase diagram of UIr is shown in Figure 5. The transition temperatures T_{C1} obtained from the present study are indicated by circles. The phase boundaries indicated by solid lines are determined by the resistivity and dc magnetization measurements; the ones indicated by broken lines are determined by ac susceptibility measurements.¹⁹ The superconducting region is indicated by a shadow at an enlarged scale. It is found that the pressure dependence of T_{C1} determined by the present heat capacity measurement is consistent with those determined in the previous study. The temperatures where C_{ac} shows bending are indicated by squares. Interestingly, these temperatures are close to the boundary of the FM3 phase. Thus, the bending anomaly may be the thermodynamic one related of the phase boundary of the FM3 phase. The anomaly does not appear in C_{ac} at 2.61 GPa where the value of T_{C3} is estimated to be approximately 5 K from the previous studies.¹⁹ The reason for the absence of the heat capacity anomaly is not clear. One possibility is that the critical pressure of the FM3 phase in the present study may be different from that of previous reports due to sample dependence or ambiguity in pressure determination.

Next, we discuss the magnitude of the heat capacity

Table I. Calculated heat capacity jump

$P(\text{GPa})$	T_m (K)	$\Delta C/T_m^{(\text{SCR})}$ (mJ/K ² ·mol)	$\Delta C/T_m^{(\text{Stoner})}$ (mJ/K ² ·mol)
0	$T_{C1} = 46$ K	11	44
1.8	$T_{C2} = 13$ K	0.11	0.44
2.2	$T_{C3} = 14$ K	0.22	0.88
2.4	$T_{C3} = 10$ K	0.30	1.2
2.6	$T_{C3} = 5$ K	0.6	2.4

anomaly in UIr. The heat capacity anomaly in itinerant ferromagnets has been the subject of theoretical studies.^{22–25} In the Stoner-Wohlfarth model, the jump of the heat capacity at the transition temperature was estimated as $\Delta C/T_m^{(\text{Stoner})} = (\mu_0 M_0^2)/(\chi_0 T_m^2)$, where M_0 is the spontaneous magnetization and χ_0 is the magnetic susceptibility in the ordered state. The Stoner theory does not include the effect of the spin fluctuations and the heat capacity jump is overestimated. Mohn and Hilscher derived the following expression for the heat capacity jump at the transition temperature within the frame work of the self-consistent renormalized (SCR) spin fluctuation theory based on the model by Murata and Doniach, $\Delta C/T_m^{(\text{SCR})} = (\mu_0 M_0^2)/(4\chi_0 T_m^2)$.²⁶ It should be noted that the value of $\Delta C/T_m^{(\text{SCR})}$ is 1/4 that of $\Delta C/T_m^{(\text{Stoner})}$. Mohn and Hilscher compared the experimental results of several itinerant ferromagnets with the theoretical models and found that the experimental values lay between $\Delta C/T_m^{(\text{SCR})}$ and $\Delta C/T_m^{(\text{Stoner})}$, an upper and lower bounds.²⁶

In the case of UIr, the value of $\Delta C/T_m^{(\text{SCR})}$ at ambient pressure is calculated to be 11 mJ/K²·mol, using $M_0 = 1.1 \times 10^5$ A/m and $\chi_0 = 4.0 \times 10^{-5}$, which are determined from the magnetization measurement at 1.8 K.¹⁴ From the present experiment, $\Delta C/T_m^{(\text{exp.})}$ is estimated to be 25 mJ/K²·mol. This value lies between $\Delta C/T_m^{(\text{SCR})}$ and $\Delta C/T_m^{(\text{Stoner})}$. The calculated values under pressures are listed in Table 1. In the calculations, we used the values of M_0 and χ_0 from the previous magnetization measurements under pressure.¹⁸ The spontaneous magnetic moments of the FM2 and FM3 phases are very small, approximately 0.05 μ_B /U. The calculated value of $\Delta C/T_m$ is significantly reduced in the FM2 and FM3 phases. This may be the reason that C_{ac} does not show a clear heat capacity jump but shows bending structure at T_{C3} .

4. Summary

We present our experimental results on the noncentrosymmetric superconductors CePt₃Si and UIr. The pressure phase diagrams of both these compounds are determined from the thermodynamic viewpoint. In CePt₃Si, the antiferromagnetic phase disappears at $P_{AF} \simeq 0.6$ GPa. Meanwhile, the superconducting phase exists in a wider pressure region from the ambient pressure to $P_{AF} \simeq 1.5$ GPa. The phase diagram of CePt₃Si is very unique. The superconductivity appears to be different from those observed around the magnetic quantum critical point. In UIr, the heat capacity anomaly was observed at T_{C1} and the pressure dependence of T_{C1} by the present study was consistent with that obtained in previous studies by the resistivity and magnetization measurements. C_{ac} shows bending at around T_{C3} . The weakness in the heat capacity anomaly may be due to the very small ordered moment of the FM3 phase.

5. Acknowledgements

This work was financially supported by the Grant-in-Aid for Creative Scientific Research (15GS0213), Scientific Research of Priority Areas and Scientific Research (A) from the Ministry of Education, Culture, Sports, Science and Technology (MEXT).

- 1) E. Bauer, G. Hilscher, H. Michor, Ch. Paul, E. W. Scheidt, A. Gribanov, Yu. Seropegin, H. Noël, M. Sigrist, and P. Rogl: Phys. Rev. Lett. **92** (2004) 027003.
- 2) T. Akazawa, H. Hidaka, H. Kotegawa, T. C. Kobayashi, T. Fujiwara, E. Yamamoto, Y. Haga, R. Settai, and Y. Ōnuki: J. Phys.:Condens. Matter **16** (2004) L. 29.
- 3) N. Kimura, K. Ito, K. Saitoh, Y. Umeda, H. Aoki, and T. Terashima: Phys. Rev. Lett. **95** (2005) 247004.
- 4) I. Sugitani, Y. Okuda, H. Shishido, T. Yamada, A. Thamizhavel, E. Yamamoto, T. D. Matsuda, Y. Haga, T. Takeuchi, R. Settai, and Y. Ōnuki: J. Phys. Soc. Jpn. **75** (2006) 0437003.
- 5) R. Settai, T. Takeuchi, and Y. Ōnuki: submitted.
- 6) V. P. Mineev: Int. J. of Mod. Phys. B **18** (2004) 2963.
- 7) N. Metoki, K. Kaneko, T. D. Matsuda, A. Galatanu, T. Takeuchi, S. Hashimoto, T. Ueda, T. D. Matsuda, Y. Ōnuki, and N. Bernhoeft: J. Phys.:Condens. Matter. **16** (2004) L207.
- 8) A. Amato, E. Bauer, and C. Baines: Phys. Rev. B **71** (2005) 092501.
- 9) W. Higemoto, Y. Haga, T. D. Matsuda, Y. Ōnuki, K. Ohishi, T. U. Ito, A. Koda, S. R. Saha, and R. Kadono: J. Phys. Soc. Jpn. **75** (2006) 124713.
- 10) M. Yogi, Y. Kitaoka, S. Hashimoto, T. Yasuda, R. Settai, Y. Ōnuki, P. Rogl, and E. Bauer: Phys. Rev. Lett. **93** (2004) 027003.
- 11) M. Yogi, H. Mukuda, Y. Kitaoka, S. Hashimoto, T. Yasuda, R. Settai, T. D. Matsuda, Y. Haga, Y. Ōnuki, P. Rogl, and E. Bauer: J. Phys. Soc. Jpn. **75** (2006) 013709.
- 12) T. Yasuda, H. Shishido, T. Ueda, S. Hashimoto, R. Settai, T. Takeuchi, T. D. Matsuda, Y. Haga, and Y. Ōnuki: J. Phys. Soc. Jpn. **73** (2004) 1657.
- 13) A. Dommann, F. Hullinger, T. Siegrist and P. Fischer: J. Magn. Mater. **67** (1987) 323.
- 14) A. Galatanu, Y. Haga, E. Yamamoto, T. D. Matsuda, S. Ikeda, and Y. Ōnuki: J. Phys. Soc. Jpn. **73** (2004) 766.
- 15) E. Yamamoto, Y. Haga, H. Shishido, H. Nakawaki, Y. Inada, R. Settai, and Y. Ōnuki: Physica B **312-313** (2002) 302.
- 16) E. Yamamoto, Y. Haga, T. D. Matsuda, A. Nakamura, R. Settai, Y. Inada, H. Sugawara, H. Sato, Y. Ōnuki: J. Nucl. Sci. Technol. suppl. **3** (2002) 187.
- 17) E. D. Bauer, E. J. Freeman, C. Sirvent, and M. B. Maple: J. Phys.: Condens. Matter **13** (2001) 5675.
- 18) T. Akazawa, H. Hidaka, H. Kotegawa, T. C. Kobayashi, T. Fujiwara, E. Yamamoto, Y. Haga, R. Settai, and Y. Ōnuki: J. Phys. Soc. Jpn. **73** (2004) 3129.
- 19) T. C. Kobayashi, S. Fukushima, H. Hidaka, H. Kotegawa, T. Akazawa, E. Yamamoto, Y. Haga, R. Settai, Y. Ōnuki: Physica B **378-380** (2006) 355.
- 20) N. Tateiwa, Y. Haga, T. D. Matsuda, S. Ikeda, T. Yasuda, T. Takeuchi, R. Settai, and Y. Ōnuki: J. Phys. Soc. Jpn. **74** (2005) 1903.
- 21) J. Flouquet: *Progress in Low Temperature Physics*, ed. B. Halperin (Elsevier, 2005), Vol. **XV**, Chap. 2.
- 22) E. P. Wohlfarth: Physica B & C **91** (1977) 305.
- 23) T. Moriya: *Spin Fluctuations in Itinerant Electron Magnetism*, (Springer-Verlag, Berlin, 1985).
- 24) K. K. Murata and S. Doniach: Phys. Rev. Lett. **29** (1972) 285.
- 25) G. G. Lonzarich and L. Taillefer: J. Phys. C **18** (1985) 4339.
- 26) P. Mohn and G. Hilscher: Phys. Rev. B **40** (1989) 9126.